Journal of Applied Mechanical Engineering
ISSN: 2168-9873

Elmarakbi et al., J Appl Mech Eng 2013, 2:4
DOI: 10.4172/2168-9873.1000128

Research Article Open Access

Under Pitch Control Techniques for Crashworthiness Improvement: Analytical Approach Using IHBM for Vehicle Control System and Extendable Structure

Ahmed Elmarakbi[1]*, Mustafa Elkady[1,2] and John Davies[1]

[1]*Department of Computing, Engineering and Technology, University of Sunderland, Sunderland, UK*
[2]*Department of Automotive Engineering, Faculty of Engineering, Ain Shams University, Cairo, Egypt*

Abstract

The aim of this paper is to improve vehicle crashworthiness using vehicle dynamics control systems (VDCS) integrated with an extendable front-end structure (extendable bumper). The work carried out in this paper includes developing and analyzing a new vehicle dynamics/crash mathematical model in case of vehicle-to-vehicle full frontal impact. This model integrates a vehicle dynamics model with the vehicle's front-end structure to define the vehicle body crash kinematic parameters. In this model, the anti-lock braking system (ABS) and the active suspension control system (ASC) are co-simulated, and its associated equations of motion are developed and solved using Incremental Harmonic Balance Method (IHBM). An Under Pitch Control (UPC) technique is used to minimize the deformation zone, pitch angle and its acceleration. The simulations show considerable improvements using UPC alongside ABS with and without the extendable bumper (EB), which produces additional significant improvements for both vehicle boy acceleration and intrusion.

Keywords: Crashworthiness improvement; Vehicle dynamics control system; Extendable bumper; Mathematical modelling; IHBM

Introduction

The increasing public awareness of safety issues and the increasing legislative requirements have increased the pressure on vehicle manufacturers to improve the vehicle crashworthiness. Accident analyses have shown that two-thirds of the collisions in which car occupants have been injured are frontal collisions [1,2]. Despite worldwide advances in research programs to develop intelligent safety systems, frontal collision remains to be the major source of road fatalities and serious injuries for decades to come [3]. The evaluation of the deformation behaviour of the front-end of passenger vehicles has been based on the assumption that in frontal collisions, the kinetic energy of the vehicle should be transformed into plastic deformation with a minimum deformation of the vehicle [4].

Many different techniques were studied to investigate the opportunities of the vehicle collision mitigation. These techniques can be classified as pre and post-collision. The most well-known pre-collision method is the advance driver assistant systems (ADAS). The aim of ADAS is to mitigate and avoid vehicle frontal collisions. The main idea of ADAS is to collect data from the road (i.e. traffic lights, other cars distances and velocities, obstacles etc.) and transfer this information to the driver, warn the driver in danger situations and aide the driver actively in imminent collision. There are different actions may be taken when these systems detect that the collision is unavoidable. For example, the brake assistant system (BAS) [5] and the collision mitigation brake system (CMBS) [6] were used to activate the braking instantly based on the behaviour characteristics of the driver, and relative position from the most dangerous other object for the moment. While ADAS was investigated, developed, and already used for some modern vehicles, it is still far away from its goal to prevent vehicle collisions.

In terms of the enhancing crash energy absorption and minimizing deformation of the vehicle's structure in post-collision, two types of smart front-end structures, namely: extendable and fixed, have been proposed and analysed to mitigate vehicle collision and enhance crash behaviour in different crash scenarios [7-12]. The extendable smart front-end structure, which is considered in this paper, consists of two hydraulic cylinders integrated with the front-end longitudinal members of standard vehicles. The hydraulic cylinders can be extended in impending collisions using radar techniques to absorb the impact kinetic energy proving that smart structure can absorb more crash energy by their damping characteristics. For this smart structure, several mathematical models were developed and analytical and numerical simulations were presented [7-12].

In the same way an extendable and retractable knee bolster was mathematically presented [13]. This can be extended at the threat of impending collision and retracted if the threat is suppressed. This system was proposed to be positioned in the lower portion of the instrument panel of a vehicle at knee height to an occupant. Another extendable and retractable bumper (E/R bumper) was presented analytically and experimentally [14]. Also the E/R bumper extends at impending collision to give an extra gap for absorption of crush energy and retracts when the threat disappears. This system provides a maximum bumper extension of 100 mm which is suitable for a maximum crash speed of about 60 km/hr.

Modern motor vehicles are increasingly using vehicle dynamic control systems (VDCS) to replace traditional mechanical systems in order to improve vehicle handling, stability, and comfort. In addition, VDCS are playing an important role for active safety system for road

***Corresponding author:** Ahmed Elmarakbi, Department of Computing, Engineering and Technology, University of Sunderland, Sunderland SR6 0DD, UK, Tel: +44 (191) 515-3877; E-mail: ahmed.elmarakbi@sunderland.ac.uk

Received September 18, 2013; **Accepted** November 15, 2013; **Published** November 20, 2013

Citation: Elmarakbi A, Elkady M, Davies J (2013) Under Pitch Control Techniques for Crashworthiness Improvement: Analytical Approach Using IHBM for Vehicle Control System and Extendable Structure. J Appl Mech Eng 2: 128. doi:10.4172/2168-9873.1000128

vehicles, which control the dynamic vehicle motion in emergency situations. Anti-lock brake system (ABS) is used to allow the vehicle to follow the desired steering angle while the intense braking is applied [15]. In addition, the ABS helps reducing the stopping distance of a vehicle compared with the conventional braking system. The Active suspension control system (ASC) is used to improve the quality of the vehicle ride and reduce the vertical acceleration [16,17].

An extensive review of the current literatures showed that a little research exists on the influences of vehicle dynamics on vehicle collisions [18]. The influence of the braking force on vehicle impact dynamics in low-speed rear-end collisions has been studied [19]. It was confirmed that the braking force was not negligible in high-quality simulations of vehicle impact dynamics at low speed. The effect of vehicle braking on the crash and the possibility of using vehicle dynamics control systems to reduce the risk of incompatibility and improve the crash performance in frontal vehicle-to-barrier collision were investigated [20]. They proved that there is a slight improvement of the vehicle deformation once the brakes are applied during the crash. A multi-body vehicle dynamic model using ADAMS software, alongside with a simple crash model was generated in order to study the effects of the implemented control strategy.

In this paper a unique vehicle crash/dynamics mathematical model is developed. This model is used to investigate the mitigation of the vehicle collision in the case of full frontal vehicle-to-vehicle crash scenario using VDCS and an extendable bumper.

Mathematical Modelling

The main advantage of the mathematical modelling (using numerical and/or analytical solutions) is producing a reliable quick simulation results. The mathematical modelling tool is preferable in the first stage of design to avoid the high computational costs using Finite Element (FE) models. Two analytical models were created using a computer simulation, one for vehicle component crash and the other for barrier impact statically and then both models were merged into one model [21]. To achieve enhanced occupant safety, the crash energy management system was explored [22]. In his study, he used a simple lumped-parameter model and discussed the applicability of providing variable energy-absorbing properties as a function of the impact speed.

In this paper, 8-Degree- of- Freedom (DoF) vehicle dynamics/crash mathematical models is developed to study the effect of vehicle dynamics control systems on vehicle collision mitigation. Full frontal vehicle-to-vehicle crash scenario is considered in this study.

As shown in Figure 1, vehicle "**a**" represents the vehicle equipped with extendable front-end structure and vehicle "**b**" represents the existing standard vehicle. The impact initial velocities of both vehicle "**a**" and vehicle "**b**" are v_a and v_b, respectively.

In this model, the vehicle body is represented by lumped mass m and it has a translational motion on longitudinal direction (x-axis), translational motion on vertical direction (z-axis) and pitching motion (around y-axis). The front-end structure is represented by two non-linear springs with stiffness's k_{su} and k_{sl} for the upper members (rails) and the lower members of the vehicle frontal structure, respectively. The hydraulic cylinders, with length l_g, are represented by dampers with damping coefficient C_b. The cross members (vehicle "a") and the bumper are represented by lumped masses m_{cm} and m_{ca}, respectively, and they only have a longitudinal motion in x direction. The bumper of vehicle "**b**" is represented by m_{cb}. It is worthwhile noting that in the case of vehicle-to-vehicle frontal collision, the masses of the two bumpers (bumpers assembly), m_{ca} and m_{cb}, are assumed to be in contact throughout the crash process and have the same velocity and displacement in longitudinal x direction. The mass of the two bumpers are defined by m_c and provides a mechanism of load transfer from one longitudinal to the other.

The ABS and the ASC systems are co-simulated with a vehicle dynamic model and integrated with a non-linear front-end structure model combined with an extendable bumper as shown in Figure 1. The general dimensions of the model are shown in Figure 1, where l_f, l_r, h, e_1 and e_2 represent the longitudinal distance between the vehicle's centre of gravity (CG) and front wheels, the longitudinal distance between the CG and rear wheels, the high of the CG from the ground, the distance between the CG and front-end upper springs and the CG and front-end lower springs respectively. At the first stage of impact, deformation of the front-end and vehicle pitching are small and only the lower members are deformed through the extendable bumper. At the end of impact the deformation of the front-end reaches its maximum level (for the upper and lower members), vehicle pitch angle increases and the rear wheels leave the ground. It is assumed that the front-end springs are still horizontal during impact, and they will not incline with the vehicle body.

Two spring/damper units are used to represent the conventional vehicle suspension systems. Each unit has a spring stiffness k_S and a damping coefficient c. The subscripts f and r, u and l denote the front and rear wheels, upper and lower longitudinal members, respectively. The ASC system is co-simulated with the conventional suspension system to add or subtract an active force element u. The ABS is co-simulated with the mathematical model using a simple wheel model. The unsprung masses are not considered in this model and it is assumed

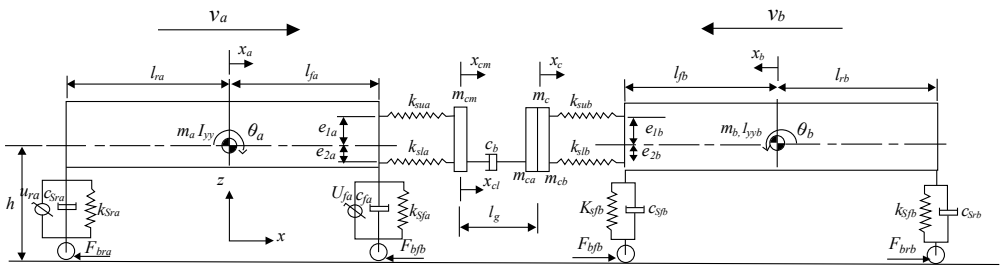

Vehciel a

(equipped with VDCS and an extendable bumper)

Vehciel b

(standard vehicle-free rolling)

Figure 1: Vehicle-to-vehicle full frontal collision.

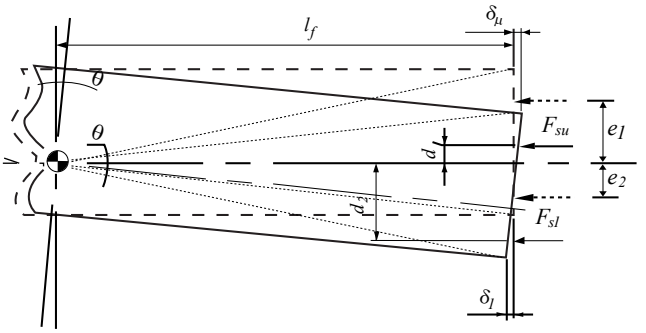

Figure 2: Illustration drawing of the front-end deformation due to vehicle pitching. (- - - Before pitching ---- After pitching).

that the vehicle moves on a flat-asphalted road, which means that the vertical movement of the tyres and road vertical forces can be neglected.

The equations of motion of the mathematical model are developed to study and predict the dynamic response of the vehicle-to-barrier in full frontal crash scenario as follows:

$$m_a \cdot \ddot{x}_a + F_{sua} + F_{sla} + F_{bfa} + F_{bra} = 0 \quad (1)$$

$$m_b \cdot \ddot{x}_b + F_{sub} + F_{slb} + F_{bfb} + F_{brb} = 0 \quad (2)$$

$$m_a \cdot \ddot{z}_a + F_{Sfa} + F_{Sra} = 0 \quad (3)$$

$$m_b \cdot \ddot{z}_b + F_{Sfb} + F_{Srb} = 0 \quad (4)$$

$$I_{yya} \cdot \ddot{\theta}_a - F_{Sfa} \cdot l_{fa} + F_{Sra} \cdot l_{ra} + F_{sua} \cdot d_{1a} - F_{sla} \cdot d_{2a} - (F_{bfa} + F_{bra}) \cdot (z_a + h_a) = 0 \quad (5)$$

$$I_{yyb} \cdot \ddot{\theta}_b - F_{Sfb} \cdot l_{fb} + F_{Srb} \cdot l_{rb} + F_{sub} \cdot d_{1b} - F_{slb} \cdot d_{2b} - (F_{bfb} + F_{brb}) \cdot (z_b + h_b) = 0 \quad (6)$$

$$m_{cm} \cdot \ddot{x}_{cm} + F_d - F_{sua} - F_{sla} = 0 \quad (7)$$

$$m_c \cdot \ddot{x}_c - F_d + F_{sub} + F_{slb} = 0 \quad (8)$$

The scripts and are the acceleration of the vehicle body in longitudinal direction and vertical directions, respectively. is the rotational pitching acceleration of the vehicle body. Subscripts *a, b,* c_m and *c* represents vehicle "**a**", vehicle "**b**", cross member of vehicle "**a**" and the two vehicle bumpers, respectively. F_s, F_S, F_b and F_d are front-end non-linear spring forces, vehicle suspension forces, braking forces and the damping force of the extendable bumper hydraulic cylinder, respectively. I_{yy} represents the mass moment of inertia of vehicle body about y-axis. d_1 and d_2 represent the distance between the CG and the upper springs force and the lower springs force for each vehicle due to pitching rotation, respectively and can be calculated using figure 2 as:

$$d_1 = \sqrt{l_f^2 + e_1^2} \cdot \sin(\tan^{-1}(\frac{e_1}{l_f}) + \theta) \quad (9)$$

$$d_2 = \sqrt{l_f^2 + e_2^2} \cdot \sin(\tan^{-1}(\frac{e_2}{l_f}) + \theta) \quad (10)$$

There are different types of forces which are applied on the vehicle body. These forces are generated by the deformation of the front-end structure and damping of the extendable bumper due to vehicle crushing, conventional suspension system due to the movement of the vehicle body, and the active control systems such as the ABS and ASC.

To simulate the upper and lower members of the vehicle front-end structure, multi-stage piecewise linear force-deformation spring characteristics are considered. The non-linear springs used in the multi-body model (ADAMS) [20] are taken to generate the *n* stage piecewise spring's characteristics [23]. The forces of the front-end springs are calculated using the general relationship between the force and deflection of a non-linear spring as follows:

$$F_{si} = k_{sij}\delta_i + F_{ij} \quad (11)$$

where k_s and δ represent the stiffness and the deflection of the front-end spring, respectively. The subscript *i* indicates the spring location (*u*: upper right spring, *l*: lower right spring) and the subscript *j* indicates different stages of the force-deformation characteristics as shown in Figure 5. The stiffness of the spring k_s and the force elements F_{ij} vary according to the different stages of the deflection δ and can be defined as follows:

$$k_{sij} = k_{si1}, \quad F_{ij} = 0 \quad 0 \le \delta < \delta_{i1} \quad (12)$$

$$k_{sij} = k_{si2}, \quad F_{ij} = (k_{si1} - k_{si2})\delta_{i1} \quad \delta_{i1} \le \delta < \delta_{i2} \quad (13)$$

$$k_{sij} = k_{si3}, \quad F_{ij} = (k_{si1} - k_{si2})\delta_{i1} + (k_{si2} - k_{si3})\delta_{i2} \quad \delta_{i2} \le \delta < \delta_{i3} \quad (14)$$

$$k_{sij} = k_{\sin}, \quad F_{si} = k_{sij}\delta_i + F_{ij} + (k_{si(n-1)} - k_{\sin})\delta_{i(n-1)} \quad \delta \ge \delta_{(n-1)} \quad (15)$$

where the deformation of the front-end springs δ_i can be calculated using figure 2 as follows:

$$\delta_{ua} = x_a - x_{cm} + \delta_{\theta ua} \quad (16)$$

$$\delta_{la} = x_a - x_{cm} - \delta_{\theta la} \quad (17)$$

$$\delta_{ua} = x_b + x_c + \delta_{\theta ub} \quad (18)$$

$$\delta_{lb} = x_b + x_c - \delta_{\theta lb} \quad (19)$$

where x_{cm} and x_c are the longitudinal displacement of the cross member, bumpers assembly, respectively. $\delta_{\theta u}$ and $\delta_{\theta l}$ represent the deflection of the front end due to pitching and can be calculated for both vehicles using Figure 2 as

$$\delta_{\theta u} = \sqrt{l_f^2 + e_1^2} \cdot \cos(\tan^{-1}(\frac{e_1}{l_f}) - \theta) - l_f \quad (20)$$

$$\delta_{\theta l} = \sqrt{l_f^2 + e_2^2} \cdot \cos(\tan^{-1}(\frac{e_2}{l_f}) + \theta) + l_f \quad (21)$$

The damping force of the extendable bumper that generated from the vehicle crash is expressed as follows:

$$F_d = c_d \cdot \dot{x}_{cl} \quad (22)$$

where c_d is the damping coefficient of the hydraulic cylinder of the extendable bumper, $\dot{x}_{cl}$ is the velocity of the lower cross member. The suspension forces are generated via vertical and pitching movements and the velocity of the vehicle body and can be written as follows:

$$F_{Sf} = k_{Sf} \cdot (z - l_f \cdot \sin\theta) + c_f(\dot{z} - l_f \cdot \dot{\theta} \cdot \cos\theta) - u_f \quad (23)$$

$$F_{Sr} = k_{Sr}(z + l_r \cdot \sin\theta) + c_r(\dot{z} + l_r \cdot \dot{\theta} \cdot \cos\theta) - u_r \quad (24)$$

where *z* and θ are the vehicle body vertical displacement and pitching angle, respectively, and $\dot{z}$ and $\dot{\theta}$ are the vehicle body vertical and pitching velocities, respectively. The ASC force elements (u) are applied in the vertical direction parallel to the existing conventional suspension system for vehicle "a". It is worth mention that vehicle "b" is in a free rolling mode in all cases.

The ABS and ASC control systems are co-simulated with the mathematical model. To calculate the braking force generated from the ABS, a simple wheel-road model is used, and its associated equation can be written as [23,24].

$$F_{bk} = \mu(\lambda) \cdot F_{zk} \tag{25}$$

where μ is the friction coefficient between the tyre and the road, λ is the tyre slip ratio, F_z is the vertical normal forces of the tyres. The subscript k indicates the wheel's location (*f*: front wheels and *r*: rear wheels). The ASC force elements are taken in parallel with the existing conventional suspension system and applied in the vertical direction. The maximum active suspension force is considered to be 2000 N on each wheel with the maximum suspension travel limit of 100 mm, taking into consideration the response time of the ASC system [25].

Analytical Approach: Incremental Harmonic Balance Method

The mathematical model shown in Figure 1 is used to obtain the dynamic response of the two vehicles involved in frontal full collision. The equations of motion (1-8) can be described in general by ordinary nonlinear differential equations of the matrix form:

$$M.\ddot{X} + (C_L + C_{NL}).\dot{X} + (K_L + K_{NL}).X = F \tag{26}$$

where $\ddot{\mathbf{x}}$, $\dot{\mathbf{x}}$, and X are the N×1 acceleration, velocity and displacement vectors, respectively. N is the number of degree of freedoms for the models in **M, C_L, C_{NL}, K_L, K_{NL}, F** are mass, linear damping, cubic nonlinear damping, linear stiffness, cubic nonlinear stiffness and force matrices, respectively.

There is no known general solution of the nonlinear equation of motion in Equation (26). The purpose of this section is to describe a method that can be used to find the analytical solution of Equation (26). One of the most popular methods for approximating the solutions of Equation (26) is known as Incremental Harmonic Balance Method (IHB). The IHB method was developed by [26]. The IHB method was successfully applied to various types of non-linear structural systems. Although it is valid for multi-degree-of-freedoms, the applications of this method were limited to study the steady state response with two degree-of-freedom system. Moreover, only nonlinear stiffness characteristics have been considered in the work of [26-33].

To apply the IHB method, first define time variables:

$$\tau_m = \omega_m t \quad (m = 1, 2, ..., N) \tag{27}$$

Further, two differential operators are defined:

$$\frac{d}{dt} = \sum_{m=1}^{N} \omega_m \frac{\partial}{\partial \tau_m}, \quad \frac{d^2}{dt^2} = \sum_{m=1}^{N}\sum_{n=1}^{N} \omega_m \omega_n \frac{\partial^2}{\partial \tau_m \partial \tau_n} \tag{28}$$

By using Equation (27 and 28), Equation (26) can be rewritten in the form:

$$\sum_{m=1}^{N} \omega_m \left(\sum_{n=1}^{N} \omega_n \mathrm{M} \frac{\partial^2 \mathrm{x}}{\partial \tau_m \partial \tau_n} + [\mathrm{C_L} + \mathrm{C_{NL}}(\omega_m \frac{\partial \mathrm{x}}{\partial \tau_m})] \frac{\partial \mathrm{x}}{\partial \tau_m} \right) + K_L + K_{NL}(X).X = 0 \tag{29}$$

As a first step of the IHB method, apply the Newton-Raphson iterative procedure by expressing the current solutions , as the sum of the previous solutions $\mathbf{x}_{new}$, $(\omega_m)_{new}$ and the previous solutions X, ω_m and the solution increments Δx, $\Delta\omega_m$ as

$$\mathbf{x}_{new} = \mathbf{x} + \Delta \mathbf{x} \tag{30}$$

$$(\omega_m)_{new} = \omega_m + \Delta\omega_m \tag{31}$$

Eq. (29) can be rewritten using Eqs. (30) and (31) as

$$\sum_{m=1}^{N} (\omega_m + \Delta\omega_m) \left(\sum_{n=1}^{N} (\omega_n + \Delta\omega_n) \mathrm{M} \frac{\partial^2 (\mathrm{x} + \Delta \mathrm{x})}{\partial \tau_m \partial \tau_n} + [C_L + C_{NL}((\omega_m + \Delta\omega_m) \frac{\partial (\mathrm{x} + \Delta \mathrm{x})}{\partial \tau_m})] \frac{\partial (\mathrm{x} + \Delta \mathrm{x})}{\partial \tau_m} \right) + [K_L + K_{NL}(\mathrm{x} + \Delta \mathrm{x})](\mathrm{x} + \Delta \mathrm{x}) = 0 \tag{32}$$

The nonlinear matrix differential equation (30) can be linearized by expanding its terms in Taylor series about its initial solution, keeping only linear terms of increments in the series expansion:

$$\sum_{m=1}^{N} \omega_m \left(\sum_{n=1}^{N} \omega_n \mathrm{M} \frac{\partial^2 \Delta \mathrm{x}}{\partial \tau_m \partial \tau_n} + \left[\mathrm{C_L} + \frac{\partial}{\partial \dot{\mathrm{x}}} [\mathrm{C_{NL}}(\omega_m \frac{\partial \mathrm{x}}{\partial \tau_m}) . \frac{\partial \mathrm{x}}{\partial \tau_m}] \right] \frac{\partial \Delta \mathrm{x}}{\partial \tau_m} \right) + \left[\mathrm{K_L} + \frac{\partial}{\partial \mathrm{x}} [\mathrm{K_{NL}}(\mathrm{x}).\mathrm{x}] \right] \Delta \mathbf{x} =$$

$$- \sum_{m=1}^{N} \omega_m \left(\sum_{n=1}^{N} \dot{u}_n \mathrm{M} \frac{\partial^2 \mathrm{x}}{\partial \dot{\delta}_m \partial \dot{\delta}_n} + \left[\mathrm{C_L} + \mathrm{C_{NL}}(\dot{u}_m \frac{\partial \mathrm{x}}{\partial \dot{\delta}_m}) \right] \frac{\partial \mathrm{x}}{\partial \tau_m} \right) - [\mathrm{K_L} + \mathrm{K_{NL}}(\mathrm{x})] \, . \, \mathrm{x}$$

$$- \sum_{m=1}^{N} \Delta\omega_m \left(\sum_{n=1}^{N} 2\omega_n \mathrm{M} \frac{\partial^2 \mathrm{x}}{\partial \tau_m \partial \tau_n} + \mathrm{C_L} . (\frac{\partial \mathrm{x}}{\partial \dot{\delta}_m}) + \frac{\partial}{\partial \dot{u}_m} [\mathrm{C_{NL}}(\dot{u}_m \frac{\partial \mathrm{x}}{\partial \dot{\delta}_m}) . \dot{u}_m \frac{\partial \mathrm{x}}{\partial \dot{\delta}_m}] \right) \tag{33}$$

Eq. (31) is a linear matrix differential equation in terms of unknown vector Δx, which represents the increments of vector **x** in the Newton-Raphson iterative procedure. The initial solution of vector **x** and its increment Δx can be assumed by the following equation:

$$\mathrm{x} = \mathrm{Hz}\ , \Delta \mathrm{x} = \mathrm{H} \Delta \mathrm{z} \tag{34}$$

$$\text{where } \mathrm{H} = \begin{bmatrix} \mathrm{h} & 0 & \dots & 0 \\ 0 & \mathrm{h} & \dots & 0 \\ \vdots & \vdots & \ddots & \vdots \\ 0 & 0 & \cdots & \mathrm{h} \end{bmatrix}, \ \mathrm{z} = \begin{bmatrix} \mathrm{z}_1 \\ \mathrm{z}_2 \\ \vdots \\ \mathrm{z}_N \end{bmatrix}, \text{ and } \Delta \mathrm{z} = \begin{bmatrix} \Delta \mathrm{z}_1 \\ \Delta \mathrm{z}_2 \\ \vdots \\ \Delta \mathrm{z}_N \end{bmatrix} \tag{35}$$

and the matrices **h**, **z** and Δz are defined as following

$$\mathrm{h} = \left[\sin\tau_1, \sin 3\tau_1, \ldots, \quad \sin\tau_2, \sin 3\tau_2, \ldots, \quad \cdots \quad \sin\tau_N, \sin 3\tau_N, \ldots \right] \tag{36}$$

$$\mathrm{z} = \left[b_{11}, b_{12}, \ldots, \quad b_{21}, b_{22}, \ldots, \quad \cdots \quad b_{N1}, b_{NN}, \ldots \right]^T \tag{37}$$

$$\Delta \mathrm{z} = \left[\Delta b_{11}, \Delta b_{12}, \ldots, \quad \Delta b_{21}, \Delta b_{22}, \ldots, \quad \cdots \quad \Delta b_{N1}, \Delta b_{NN}, \ldots \right]^T \tag{38}$$

Consequently, the initial solution of vectors $\dot{\mathbf{x}}$, $\ddot{\mathbf{x}}$ and their increment $\Delta\dot{\mathbf{x}}$ and $\Delta\ddot{\mathbf{x}}$ are given by

$$\dot{\mathrm{x}} = \dot{\mathrm{H}}\mathrm{z}\ , \quad \ddot{\mathrm{x}} = \ddot{\mathrm{H}}\mathrm{z}\ , \quad \Delta\dot{\mathrm{x}} = \dot{\mathrm{H}}\Delta\mathrm{z}\ , \quad \Delta\ddot{\mathrm{x}} = \ddot{\mathrm{H}}\Delta\mathrm{z} \tag{39}$$

Using Eqs. (30) and (34), the new solution of vector $\mathbf{z}_{new}$ are determined as

$$\mathbf{z}_{new} = \mathbf{z} + \Delta\mathbf{z} \tag{40}$$

Let the following matrices $\mathrm{K_{NL}}(\mathrm{x})$, $\frac{\partial}{\partial \mathrm{x}}[\mathrm{K_{NL}}(\mathrm{x}).\mathrm{x}]$, $\frac{\partial}{\partial \dot{\mathrm{x}}}[\mathrm{C_{NL}}(\omega_m \frac{\partial \mathrm{x}}{\partial \tau_m}) . \frac{\partial \mathrm{x}}{\partial \tau_m}]$, $\mathrm{C_{NL}}(\dot{u}_m \frac{\partial \mathrm{x}}{\partial \dot{\delta}_m})$, and $\frac{\partial}{\partial \dot{u}_m}[\mathrm{C_{NL}}(\dot{u}_m \frac{\partial \mathrm{x}}{\partial \dot{\delta}_m}) . \dot{u}_m \frac{\partial \mathrm{x}}{\partial \dot{\delta}_m}]$ simply denoted by $\mathrm{K_{NL}}$, $\mathrm{K_{NL1}}$, $\mathrm{C_{NL1}}$, $\mathrm{C_{NL}}$, and $\mathrm{C_{NL2}}$, respectively. Moreover, substituting Eq. (34) into Eq. (33) yields

$$\left[\sum_{m=1}^{N}\omega_m\left(\sum_{n=1}^{N}\dot{u}_n\mathrm{M}\frac{\partial^2\mathrm{H}}{\partial\hat{o}_m\partial\hat{o}_n}+\left[\mathrm{C_L}+\mathrm{C_{NL1}}\right]\frac{\partial\mathrm{H}}{\partial\hat{o}_m}\right)+\left[\mathrm{K_L}+\mathrm{K_{NL1}}\right].\mathrm{H}\right].\Delta z=$$

$$-\left[\sum_{m=1}^{N}\omega_m\left(\sum_{n=1}^{N}\dot{u}_n\mathrm{M}\frac{\partial^2\mathrm{H}}{\partial\hat{o}_m\partial\hat{o}_n}+\left[\mathrm{C_L}+\mathrm{C_{NL}}\right]\frac{\partial\mathrm{H}}{\partial\tau_m}\right)+\left[\mathrm{K_L}+\mathrm{K_{NL}}\right].\mathrm{H}\right].z-$$

$$\left[\sum_{m=1}^{N}\Delta\omega_m\left(\sum_{n=1}^{N}2\omega_n\mathrm{M}\frac{\partial^2\mathrm{H}}{\partial\tau_m\partial\tau_n}+\mathrm{C_L}.\left(\frac{\partial\mathrm{H}}{\partial\hat{o}_m}\right)+\mathrm{C_{NL2}}\right)\right].z \quad (41)$$

As a second step of the IHB method, solve Eq. (41) for the vector . This is performed by applying the Galerkin procedure.

$$\left(\int_0^{\tau_N}\cdots\int_0^{\tau_2}\int_0^{\tau_1}\left\{\mathrm{H^T}.\left[\sum_{m=1}^{N}\dot{u}_m\left(\sum_{n=1}^{N}\dot{u}_n\mathrm{M}\frac{\partial^2\mathrm{H}}{\partial\hat{o}_m\partial\hat{o}_n}+\left[\mathrm{C_L}+\mathrm{C_{NL1}}\right]\frac{\partial\mathrm{H}}{\partial\hat{o}_m}\right)+\left[\mathrm{K_L}+\mathrm{K_{NL1}}\right].\mathrm{H}\right]\right\}.\mathrm{d}\tau_1\mathrm{d}\tau_2\cdots\mathrm{d}\tau_N\right).\Delta z=$$

$$-\left(\int_0^{\tau_N}\cdots\int_0^{\tau_2}\int_0^{\tau_1}\left\{\mathrm{H^T}.\left[\sum_{m=1}^{N}\dot{u}_m\left(\sum_{n=1}^{N}\dot{u}_n\mathrm{M}\frac{\partial^2\mathrm{H}}{\partial\hat{o}_m\partial\hat{o}_n}+\left[\mathrm{C_L}+\mathrm{C_{NL}}\right]\frac{\partial\mathrm{H}}{\partial\hat{o}_m}\right)+\left[\mathrm{K_L}+\mathrm{K_{NL}}\right].\mathrm{H}\right]\right\}.\mathrm{d}\tau_1\mathrm{d}\tau_2\cdots\mathrm{d}\tau_N\right).z$$

$$-\left(\int_0^{\tau_N}\cdots\int_0^{\tau_2}\int_0^{\tau_1}\left\{\mathrm{H^T}.\left[\sum_{m=1}^{N}\Delta\omega_m\left(\sum_{n=1}^{N}2\dot{u}_n\mathrm{M}\frac{\partial^2\mathrm{H}}{\partial\hat{o}_m\partial\hat{o}_n}+\mathrm{C_L}\frac{\partial\mathrm{H}}{\partial\tau_m}\right)\right.\right.\right.$$

$$\left.\left.\left.\cdot\mathrm{C_{NL2}}\right]\right\}.\mathrm{d}\tau_1\mathrm{d}\tau_2\cdots\mathrm{d}\tau_N\right).z \quad (42)$$

Eq. (42) can be rewritten in a simple form of a linear algebraic matrix equation system for unknown vector as follows:

$$A.\Delta z=R-\sum_{m=1}^{N}\Delta\omega_m.Q_m \quad (43)$$

The matrix **A** is composed from linear and nonlinear part:

$$\mathrm{A}=\mathrm{A_L}+\mathrm{A_{NL}} \quad (44)$$

where

$$\mathrm{A_L}=\int_0^{\tau_N}\cdots\int_0^{\tau_2}\int_0^{\tau_1}\left[\sum_{m=1}^{N}\dot{u}_m\left(\sum_{n=1}^{N}\dot{u}_n\mathrm{H^T}\mathrm{M}\frac{\partial^2\mathrm{H}}{\partial\hat{o}_m\partial\hat{o}_n}+\mathrm{H^T}\mathrm{C_L}\frac{\partial\mathrm{H}}{\partial\tau_m}\right)+\mathrm{H^T}\mathrm{K_L}\mathrm{H}\right].\mathrm{d}\tau_1\mathrm{d}\tau_2\cdots\mathrm{d}\tau_N \quad (45)$$

is the linear part and

$$\mathrm{A_{NL}}=\int_0^{\tau_N}\cdots\int_0^{\tau_2}\int_0^{\tau_1}\left[\sum_{m=1}^{N}\omega_m\mathrm{H^T}\mathrm{C_{NL1}}\frac{\partial\mathrm{H}}{\partial\hat{o}_m}+\mathrm{H^T}\mathrm{K_{NL1}}\mathrm{H}\right].\mathrm{d}\tau_1\mathrm{d}\tau_2\cdots\mathrm{d}\tau_N \quad (46)$$

is the nonlinear part of the matrix **A**

and the matrix **R** is given by

$$\mathrm{R}=\int_0^{\tau_N}\cdots\int_0^{\tau_2}\int_0^{\tau_1}\mathrm{H^T}\mathrm{F}\,\mathrm{d}\tau_1\mathrm{d}\tau_2\cdots\mathrm{d}\tau_N-\mathrm{A_L}\cdot z+\mathrm{R_{NL}} \quad (47)$$

where

$$\mathrm{R_{NL}}=-\left(\int_0^{\tau_N}\cdots\int_0^{\tau_2}\int_0^{\tau_1}\left[\sum_{m=1}^{N}\omega_m\mathrm{H^T}\mathrm{C_{NL}}\frac{\partial\mathrm{H}}{\partial\hat{o}_m}+\mathrm{H^T}\mathrm{K_{NL}}\mathrm{H}\right].\mathrm{d}\tau_1\mathrm{d}\tau_2\cdots\mathrm{d}\tau_N\right).z \quad (48)$$

is the nonlinear part of the matrix

Likewise, the matrix $\mathrm{Q_m}$ decomposed into linear $\mathrm{Q_{mL}}$ and nonlinear part $\mathrm{Q_{mNL}}$ as follows:

$$\mathrm{Q_{mL}}=-\left(\int_0^{\tau_N}\cdots\int_0^{\tau_2}\int_0^{\tau_1}\left[\sum_{n=1}^{N}2\dot{u}_n\mathrm{H^T}\mathrm{M}\frac{\partial^2\mathrm{H}}{\partial\hat{o}_m\partial\hat{o}_n}+\mathrm{H^T}\mathrm{C_L}\frac{\partial\mathrm{H}}{\partial\tau_m}\right].\mathrm{d}\tau_1\mathrm{d}\tau_2\cdots\mathrm{d}\tau_N\right).z \quad (49)$$

$$\mathrm{Q_{mNL}}=-\left(\int_0^{\tau_N}\cdots\int_0^{\tau_2}\int_0^{\tau_1}\left[\mathrm{H^T}\frac{\partial}{\partial\dot{u}_m}[\mathrm{C_{NL}}(\dot{u}_m\frac{\partial\mathrm{x}}{\partial\hat{o}_m}).\dot{u}_m\frac{\partial\mathrm{x}}{\partial\hat{o}_m}]\right].\mathrm{d}\tau_1\mathrm{d}\tau_2\cdots\mathrm{d}\tau_N\right).z \quad (50)$$

The matrices **h**, **z** and $\Delta\mathbf{z}$ can be defined from Eqs. (36-38) with two degree of freedom, N=2. The solution starts by assuming initial values of vector **z**. Then matrices **A** and **R** are computed using Eqs. (44) and (47), respectively. Thus, the unknown vector $\Delta\mathbf{z}$ is computed from Eq. (43) at constant frequency ω ($\Delta\omega=0$). Once $\Delta\mathbf{z}$ is known, the new solution $\mathbf{z}_{new}$ is obtained by means of Eq. (40). This process is repeated iteratively using the Newton-Raphson procedure until the convergent solution is reached. Finally, the vector **x** can be obtained from Eq. (34).

Simulations

In this section, the analysis developed in the former sections is verified by the presentation of the simulation results. Two sets of analysis are carried out in this section. The first set includes a full frontal impact between vehicle "**b**" (standard vehicle in a free rolling scenario) and vehicle "**a**" (equipped with the extendable bumper and VDCS). The VDCS in the case includes anti-lock braking system (ABS) integrated with under-pitch control (UPC) technique. The UPC is developed with the aid of the ASC system using the fuzzy logic controller. The idea of the UPC controller technique is to give the vehicle body negative pitch angle before the crash and try to maintain the vehicle in this case until it collides with the other vehicle. The objective of the UPC system is to obtain the minimum pitching angle and acceleration of the vehicle body during the crash.

The second set of analysis also includes a full frontal impact between vehicle "**b**" (standard vehicle in a free rolling scenario) and vehicle "**a**" (equipped only with VDCS). The VDCS in the case includes anti-lock braking system (ABS) integrated with under-pitch control (UPC). The extendable bumper won't be used in this case to clarify the VDCS effects on the collision mitigation.

While the ADAS detected that the crash is unavoidable at 1.5 sec prior to the impact [34], the VDCS and the extendable bumper will be activated in this short time prior the impact. The values of different parameters used in numerical simulations are given in Table 1 [35]; while the damping coefficient and the length of the hydraulic cylinder of the extendable bumper system are chosen to be 20000 N.s/m, and 0.4 m, respectively. The vehicles are adapted to collide with each other with the same velocity of 55 km/hr. Prior collisions, the front-springs forces are equal to zero in the equations of motion. The front-end springs forces are re-deactivated at the end of collision (vehicle's velocity equal zero/negative values) and the behaviour of the vehicle in post-collision is captured.

It is worth mentioning that the developed vehicle dynamics/crash

Parameter	m	I_{yy}	k_{Sf}	k_{SfR}	$c_{fR=cfL}$	$c_{rR=crL}$	l_f	l_r
Value	1200 kg	1490 kg.m^2	36.5 kN/m	27.5 kN/m	1100 N.s/m	900 N.s/m	1.185 m	1.58 m

Table 1: Values of different parameters used in simulations for both vehicles (Alleyne, 1997).

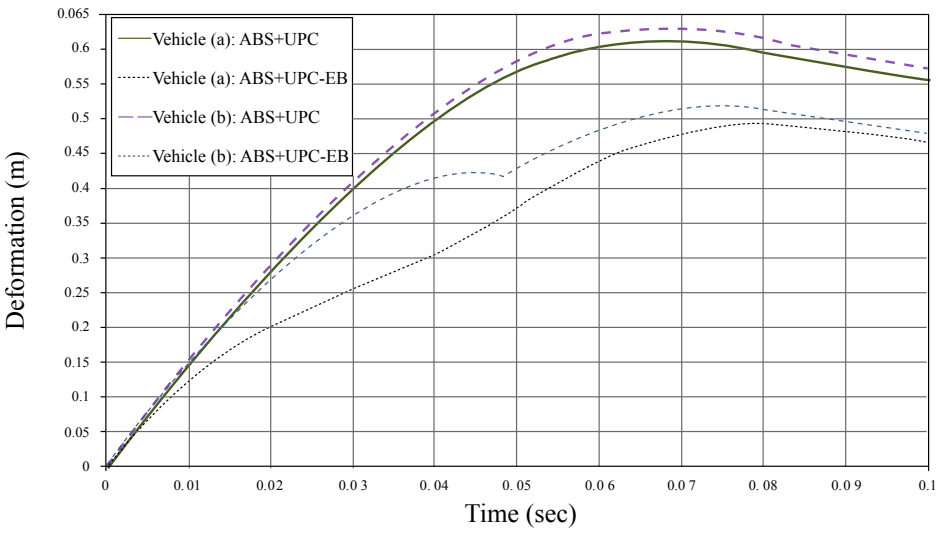

Figure 3: Deformation of the front-end structure.

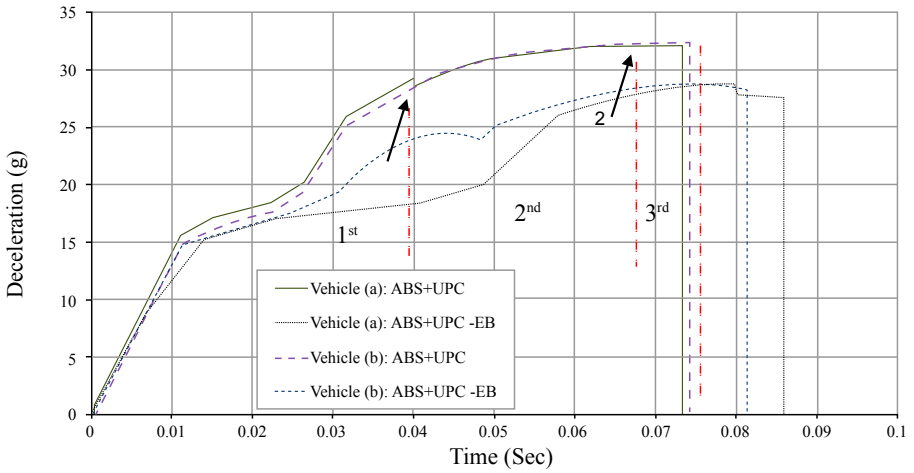

Figure 4: Vehicle body deceleration.

model has been validated to determine if the 8-DOF mathematical model provides a valid measure of vehicle response [25]. This is accomplished by comparing the mathematical model results with real test data and the results of the former ADAMS model [36].

Front-end deformation, vehicle body acceleration, pitching angle and its acceleration are depicted as main criteria to assess the crash behaviour of both vehicles.

The following results compare the dynamic response and crash response of the two vehicles involved in a full frontal collision for both sets of analysis defined early. Figure 3 shows the front-end structure's deformation-time histories for both vehicles. It is noticed that when the extendable bumper is not used, the deformation increased to reach its maximum value and then decreased slightly due to front-end springs rebound. A reduction of about 20 mm of the maximum deformation is obtained in vehicle "**a**" compared with vehicle "**b**". When the extendable bumper is applied to vehicle a, the deformation of the front-end increased slowly to reach a specific point (at around 0.05 sec); at this point the extendable bumper is completely deformed. Then the deformation increased rapidly to reach its maximum value and then decreased slightly due to the rebound effect.

The fundamental advantage of the extendable bumper is to absorb more crash energy by the ability of use more distance available for crush. Therefore, the significant reduction in the front-end deformation shown in Figure 3 is logic. The effect of UPC system helps also reducing the deformation of vehicle "**a**", and it becomes more efficient when the extendable bumper is applied. The reduction of the maximum deformation is increased to be about 25 mm compared with vehicle "**b**", which is greater than the reduction obtained without the use of the extendable bumper.

The deceleration-time histories of both vehicles are illustrated in Figure 4. Without using the extendable bumper, the deceleration-time history can be divided to three stages. The first stage represents the increase of the vehicle's deceleration before the front wheels reach the other vehicle. In this stage, a slight higher deceleration is noticed

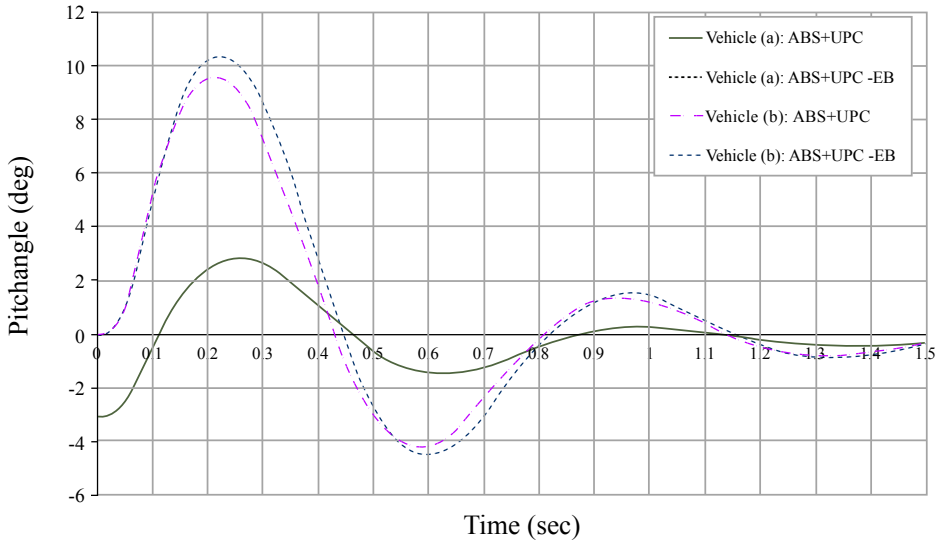

Figure 5: Vehicle body pitch angle.

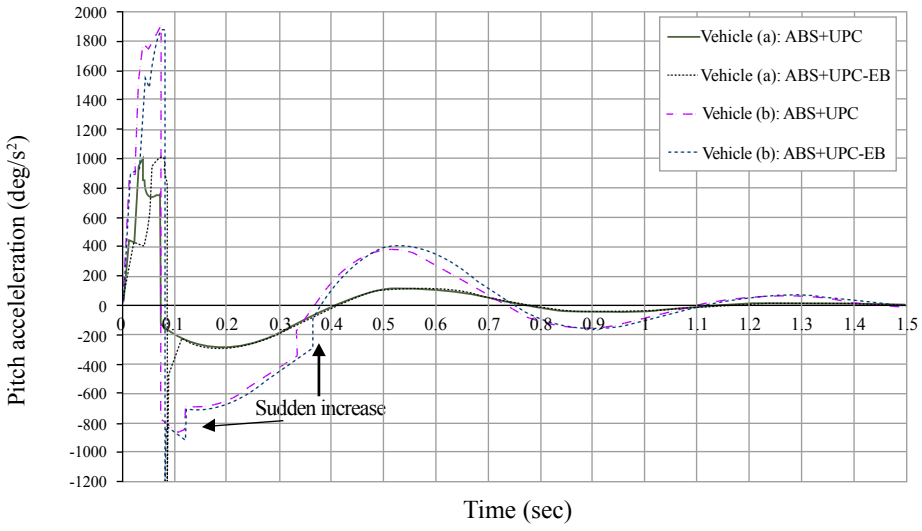

Figure 6: Vehicle body pitch acceleration.

for vehicle "**a**" due to the application of the ABS. In the second stage, the frontal wheels reach the other vehicle and stop moving; therefore their braking effects are vanished. At the beginning of this stage a rapid reduction in the vehicle "**a**" deceleration occurs (arrow 1, Figure 4). This drop does not appear for vehicle "**b**" because it is collided at a free rolling condition, no braking effect. At the end of this stage, the vehicle stops and starts moving in the opposite direction. In addition, the braking force changes its direction and another drop in the vehicle deceleration is noticed as also shown in Figure 4, (arrow 2). The maximum deceleration is observed in this stage and it is almost the same for both vehicles. At the third stage, a condition of allowing the front-end structure to be rebounded for a very short time is applied during the simulation analysis. During this stage, the vehicle moves back and the deformation of the front-end decreases as shown in Figure 3. At the end of this stage, the non-linear front-end springs are deactivated and the vehicle's deceleration is suddenly dropped to a value of zero. This fast drop is due to the assumption of immediate stopping the effect front-end springs after very short time of rebound.

When vehicle "**a**" is equipped with the extendable bumper, the front wheels do not reach the other vehicle; therefore, the second stage does not exist when the extendable bumper is applied. Since the point of impact until the extendable bumper is completely compressed (between 0.04 and 0.05 sec), a higher deceleration is noticed for vehicle "**b**" compared with vehicle "**a**". After this point, a rapid increase of the deceleration for both vehicles is noticed. The maximum deceleration is almost the same for both vehicles; however, the average deceleration of vehicle "**a**" is less than vehicle "**b**". It is clear from Figure 4 that the maximum deceleration for the two vehicles are low (28 g) when the extendable bumper is used compared with (32 g) when the extendable bumper is not applied. It is also obvious that the effect of the UPC system on vehicle deceleration is insignificant.

Figure 5 shows the vehicle's pitch angle-time histories for both vehicles. The UPC system is applied 1.5 second before collision, therefore, the vehicle body impacts the other vehicle at different value of pitch angles as shown in Figure 5. The vehicle's pitch angle then reaches

its maximum values (normally after the end of crash) according to the crash scenario. Following this, the pitch angle reduced to reach negative values and then bounces to reach its steady-state condition.

When the under pitch technique is applied along with ABS, the vehicle is given a negative pitch angle prior to impact, and the UPC forces generate a negative pitch moment prior and during the impact. In this case a great improvement of the vehicle pitching is obtained for vehicle "**a**". It is noticed that the use of the extendable bumper does not affect the pitching angle of vehicle "**a**", however, it affects vehicle "**b**" negatively. The pitching angle of vehicle "b" is increased by a value equal to about 0.7 deg, and this small value in fact is insignificant.

The vehicle pitch acceleration-time histories are depicted in Figure 6 for both vehicles. The pitch acceleration is increased very quickly at the early stage of the impact to reach its maximum value for each crash scenario due to the high pitching moment generated from the collision. At the end of the collision, all pitching moments due to the crash are equals to zero, vehicles speeds are negative with very low values, and the vehicle pitch angles are still positive. This means the vehicle is now controlled by the tyres and suspension forces, which have already generated moments in the opposite direction of the vehicle pitching. This describes the reason for the high drop and the changing direction from positive to negative on the vehicle pitch acceleration at the end of the crash.

As shown in the Figure 6, the vehicle's maximum pitching acceleration occurs at the end of the collision. The reduction of the vehicle pitch acceleration in this case is also notable; it decreases from about 1900 deg/s^2 in vehicle "**b**" to about 1000 deg/s^2 in vehicle "**a**". While the effect of the extendable bumper is insignificant for the maximum pitch acceleration, the mean acceleration, especially for vehicle "**a**", is reduced. The reason of this is that the pitching moment generated from the deformation of the front-end structure is low during the use of the extendable bumper. For vehicle "**b**", because of the vehicle's rear wheels left the ground during the vehicle pitching, a sudden increase of the vehicle pitching acceleration is observed when the rear wheels re-contacted the ground (look at the arrows in Figure 6). This sudden increase in pitching acceleration does not exist in vehicle "**a**" because the rear wheels do not leave the ground due to the reverse pitching moment generated from the UPC system.

Conclusions

A unique vehicle dynamics/crash mathematical model is developed to study the influences of VDCS integrated with extendable bumper system on the vehicle collision mitigation. This model combines vehicle crash structures, vehicle dynamics control and extendable bumper systems. It is shown from numerical simulations that the extendable bumper surpasses the traditional structure in absorbing crash energy at the same crash speed. Furthermore, it is shown that the extendable bumper brings significantly lower intrusions and helps keep the vehicle deceleration within desired limits. However, using the extendable bumper causes an increase in vehicle pitching angle; it does not affect the maximum pitching acceleration. The results obtained from different applied cases show that the VDCS affect the crash situation, by different ratios related to each case, positively. The deformation of the vehicle front-end structure is reduced when the VDCS is applied, and this reduction in the vehicle deformation is greater when the extendable bumper is used. The vehicle body deceleration is insignificantly changed within the applied cases of VDCS. The vehicle pitch angle and its acceleration are dramatically reduced when the ABS is applied alongside UPC system.

Acknowledgment

The authors would like to thank the Egyptian Government and the Faculty of Engineering, Ain Shams University for supporting this research. The authors also acknowledge with sadness, the contribution of Prof. Dave Crolla who has passed away during the period of this research.

References

1. Hobbes C (1991) The Need for Improved Structural Integrity in Frontal Car Impacts. 13th ESV Conference, Paris, France: 1073-1079.
2. Mizuno K, Umeda T, Yonezawa H (1997) The Relation between Car Size and Occupant Injury in Traffic Accidents in Japan.
3. Hiroyuki M (1990) A Parametric Evaluation of Vehicle Crash Performance.
4. Elsholz J (1974) Relationship between Vehicle Front-End Deformation and Efficiency of Safety Belts during Frontal Impact. 5th ESV Conference, London, England: 674-681.
5. Tamura M, Inoue H, Watanabe T, Maruko N (2001) Research on a Brake Assist System with a Preview Function.
6. Sugimoto Y, Sauer C (2005) Effectiveness Estimation Method for Advanced Driver Assistance System and its Application to Collision Mitigation Brake System.
7. Elmarakbi A, Zu J (2004) Dynamic Modelling and Analysis of Smart Vehicle Structures for Frontal Collision Improvement. International Journal of Automotive Technology 5: 247-255.
8. Elmarakbi A, Zu J (2005) Crashworthiness Improvement of Vehicle-to-Rigid Fixed Barrier in Full Frontal Impact using Novel Vehicle's Front-End Structures. International Journal of Automotive Technology 6: 491-499.
9. Elmarakbi A, Zu J (2006) Crash Analysis and Modeling of Two Vehicles in Frontal Collisions using Two Types of Smart Front-End Structures: An Analytical Approach using IHBM. International Journal of Crashworthiness 11: 467-483.
10. Elmarakbi A, Zu J (2007) Incremental Harmonic Balance Method for Analysis of Standard/Smart Vehicles-to-Rigid Barrier Frontal Collision. International Journal of Vehicle Safety 2: 288-315.
11. Elmarakbi A, Zu J (2007) Mathematical Modelling of a Vehicle Crash with Emphasis on the Dynamic Response Analysis of Extendable Cubic Nonlinear Dampers using the Incremental Harmonic Balance Method. Journal of Automobile Engineering 221: 143-156.
12. Elmarakbi A (2010) Analytical Analysis of a New Front-End Structure Offset Impact: Mass-Spring-Damper Models with Piecewise Linear Characteristics. International Journal of Vehicle Systems Modelling and Testing 5: 292-311.
13. Wang JT, Browne A (2003) Extendable and Retractable Knee Bolster. 18th International Technical Conference on the Enhanced Safety of Vehicles, ESV, Nagoya, Japan.
14. Wang J, Alan L (2005) An Extendable and Retractable Bumper. 19th International Technical Conference on the Enhanced Safety of Vehicles, ESV, Washington DC.
15. Yu F, Feng JZ, Li J (2002) A Fuzzy Logic Controller Design for Vehicle Abs with a On-Line Optimized Target Wheel Slip Ratio. International Journal of Automotive Technology 3: 165–170.
16. Yue C, Butsuen T, Hedrick J (1988) Alternative Control Laws for Automotive Active Suspensions. American Control Conference, USA: 2373 –2378.
17. Alleyne A, Hedrick JK (1995) Nonlinear Adaptive Control of Active Suspensions. IEEE Transactions on Control Systems Technology 3: 94 –101.
18. Elmarakbi A, Elkady M, El-Hage H (2013) Development of a New Crash/Dynamics Mathematical Model for crashworthiness enhancement of vehicle structures. International Journal of Crashwothiness 18: 444-458.
19. Mastandrea M, Vangi D (2005) Influence of Braking Force in Low-Speed Vehicle Collisions. Journal of Automobile Engineering 219: 151–164.
20. Hogan I, Manning W (2007) The Use of Vehicle Dynamic Control Systems for Automotive Collision Mitigation. 3rd Institution of Engineering and Technology Conference on Automotive Electronics, USA: 1 -10.
21. Kamal M (1970) Analysis and Simulation of Vehicle to Barrier Impact.
22. Khattab A (2010) Steering System and Method for Independent Steering of Wheels.

23. Elkady M, Elmarakbi A, MacIntyre J (2012) The influence of Vehicle Dynamics Control System on the Occupant's Dynamic response during a Vehicle Collision. Journal of Automobile Engineering 226: 1454-1471.

24. Ting W, Lin J (2004) Nonlinear Control Design of Anti-Lock Braking Systems Combined with Active Suspensions. 5th Asian Control Conference: 611–616.

25. Elkady M (2012) Enhancement of Vehicle Crash and Occupant Safety: A New Integrated Vehicle Dynamics Control System/Front-End Structure Mathematical Model. PhD thesis, Department of Computing, Engineering and Technology, University of Sunderland, UK.

26. Lau S, Cheuhng Y, Wu S (1982) A Variable Parameter Incrimination Method for Dynamic Instability of Linear and Nonlinear Elastic Systems. Journal of Applied Mechanics 49: 849-853.

27. Lau S, Cheuhng Y, Wu S (1983) Incremental Harmonic Balance Method with Multiple Time Scales for Periodic Vibration of Nonlinear Systems. Journal of Applied Mechanics 50: 871-876.

28. Lau S, Cheuhng Y, Wu S (1984) Nonlinear Vibration of Thin Elastic Plates. Journal of Applied Mechanics 51: 845-851.

29. Lau S, Cheuhng Y, Chen S (1989) An Alternative Perturbation Procedure of Multiple Scales for Nonlinear Dynamics Systems. Journal of Applied Mechanics 56: 667-675.

30. Lau S, Zhang W (1992) Nonlinear Vibrations of Piecewise Linear Systems by Incremental Harmonic Balance Method. Journal of Applied Mechanics 59: 153-160.

31. Lau S, Yuen S (1993) Solution Diagram of Nonlinear Dynamic Systems by IHB Method. Journal of Sound and Vibration 167: 303-316.

32. Pun D, Liu Y (2000) On the Design of the Piecewise Linear Vibration Absorber. Journal of Nonlinear Dynamics 18: 393-413.

33. Chen S, Cheung Y, Xing H (2001) Nonlinear Vibration of Plane Structures by Finite Element and Incremental Harmonic Balance Method. Journal of Nonlinear Dynamics 26: 87-104.

34. Jansson J, Gustafsson F, Jonas J (2002) Decision Making For Collision Avoidance Systems.

35. Alleyne A (1997) Improved Vehicle Performance using Combined Suspension and Braking Forces. Vehicle System Dynamics 27: 235–265.

36. Hogan I (2008) The Use of Vehicle Dynamic Control Systems for Automotive Collision Mitigation. PhD thesis, Department of Engineering and Technology, Manchester Metropolitan University, UK.